Available online at www.sciencedirect.com
SCIENCE DIRECT®
Journal of Catalysis 241 (2006) 417–425
JOURNAL OF CATALYSIS
www.elsevier.com/locate/jcat

The hydrogenation of *para*-toluidine over rhodium/silica: The effect of metal particle size and support texture

Kenneth T. Hindle, S. David Jackson *, Diane Stirling, Geoff Webb

WestCHEM, Department of Chemistry, The University of Glasgow, Glasgow G12 8QQ, Scotland

Received 13 March 2006; revised 16 May 2006; accepted 21 May 2006

Available online 21 June 2006

Abstract

The hydrogenation of *para*-toluidine was studied over a series of rhodium/silica catalysts. The reaction exhibits an antipathetic particle size effect, suggesting that plane face surface atoms, such as C_9^3 sites, are the active site for ring hydrogenation. The reaction is zero-order in *p*-toluidine and first-order in hydrogen, with the mechanism of formation of the *cis* and *trans* isomers likely through surface immine and enamine intermediates. The activation energy for the *trans* isomer (62 ± 4 kJ mol^{-1}) was systematically greater than that of the *cis* isomer (51 ± 6 kJ mol^{-1}). The support was also shown to play a part, adsorbing *trans*-4-MCYA in the early stages of the reaction, resulting in a varying *cis*:*trans* ratio. The effect of pore size was also studied; a dramatic decrease in activity was observed at pore diameters <64 Å.

Keywords: Hydrogenation; *Para*-toluidine; Rhodium/silica; Particle size effect; Kinetics; Mechanism

1. Introduction

The fine chemical industry relies heavily on traditional organic synthesis, in which catalysed reactions are often performed with homogeneous catalysts. Today, however, heterogeneous catalysts are beginning to be introduced to the fine chemical industry because of their many advantages, including separation, recovery, ease of handling and recycling, and stability [1]. Another important advantage of heterogeneous catalysis in fine chemical synthesis is the benefits to the environment. The quantity of byproducts produced in a reaction is given by the *E*-factor (kg of byproduct/kg of product). *E*-factors of <1–5 are usual for bulk chemical processes, with low values of 0.1 for some petrochemical processes. In the fine chemicals industry, values in the region of 5–50 are obtained [2]. The use of catalytic instead of stoichiometric processes reduces these values.

Alicyclic amines are important for use in pesticides, plasticizers, explosives, inhibitors of metal corrosion, and sweetening agents, and as intermediates in the pharmaceutical industry. This study investigates the hydrogenation of *p*-toluidine as an exemplar reaction for the fine chemicals industry. *p*-Toluidine was chosen for three reasons: (i) the aromatic ring can be hydrogenated, partially or fully; (ii) the $-NH_2$ group can be cleaved or can remain available for further reactions; and (iii) the methyl group adds *cis*/*trans* isomerism to the hydrogenated product.

The hydrogenation of toluidine has been rarely documented in the literature. Friefelder et al. [3] found that an alkyl substituent on the aromatic ring has very little effect on aniline hydrogenation when ruthenium dioxide is used as the catalyst. Ranade et al. [4] investigated the hydrogenation of *o*-toluidine using (*S*)-proline as a chiral auxiliary with the aim of diastereoselective hydrogenation.

Aniline hydrogenation has been more widely covered in the literature, although not to a great extent. Metal oxide catalysts have been reported for aromatic amine hydrogenation [5]; however, supported platinum, rhodium, ruthenium, and palladium, as well as cobalt and nickel, are usually the catalysts of choice [6–13]. Products reported from aniline hydrogenation include cyclohexylamine, dicyclohexylamine, *N*-phenylcyclohexylamine, diphenylamine, ammonia, benzene, cyclohexane, cyclohexanol, and cyclohexanone. The catalyst

* Corresponding author.
E-mail address: sdj@chem.gla.ac.uk (S.D. Jackson).

0021-9517/$ – see front matter
doi:10.1016/j.jcat.2006.05.019

and the reaction conditions used determine product formation and selectivity. Narayanan et al. [9,10] proposed a reaction scheme for aniline hydrogenation over Ni/Al_2O_3 and Co/Al_2O_3 catalysts in vapour-phase reactions. Ni/Al_2O_3 was more active than Co/Al_2O_3, with the major product being *N*-phenylcyclohexylamine, whereas dicyclohexylamine and cyclohexylamine were also produced. The mechanism of aniline hydrogenation over Rh/Al_2O_3 is thought to be different than that by Ni or Co supported on alumina. Work performed with a Rh/Al_2O_3 catalyst in vapour-phase hydrogenation gave cyclohexylamine and dicyclohexylamine as the two major products [11]; *N*-phenylcyclohexylamine and cyclohexane were also produced in minor amounts. It was thought that cyclohexane could be formed by the formation and subsequent hydrogenation of benzene. A comparison of supported Ni and supported Ru catalysts in liquid-phase hydrogenation showed that cyclohexylamine selectivity increased by approximately 60% in a water solvent and by 15–20% in organic solvent when changing from Ni to Ru [12]. The Ru/Al_2O_3 gave cyclohexylamine selectivity in the region of 90%. Other products produced were dicyclohexylamine, cyclohexanol, and cyclohexanone. Hydrogenations with a Rh/Al_2O_3 catalyst in a water solvent [13] gave cyclohexylamine as the main product with selectivities of 64–79%; the other products were mainly dicyclohexylamine and cyclohexanol.

This short overview highlights the differences in product selectivity depending on the catalyst and reaction conditions used. The following presents the work from the liquid-phase hydrogenation of *p*-toluidine over a series of Ru/SiO_2 catalysts, with particular emphasis on reaction kinetics and product selectivity.

2. Experimental

2.1. Catalysts

The catalysts used throughout the study were 2.5% w/w Rh/SiO_2. Davison Catalysts supplied and characterised the powder silica supports, which had a range of pore and particle sizes (Table 1). The active catalysts were prepared by Johnson Matthey by the incipient-wetness method to fill the pore volume using aqueous rhodium chloride salts. The catalysts were dried and reduced in flowing H_2/N_2. Johnson Matthey performed the catalyst characterisation. The physical properties of the active metal are also given in Table 1. The reproducibility of the rhodium surface area was $\pm 0.5\ m^2\ g^{-1}$.

2.2. Hydrogenation experiments

The hydrogenation reaction took place in a 500-cm^3 Buchi autoclave stirred tank reactor equipped with an oil heating jacket and a magnetically driven stirrer. A Buchi press-flow gas controller controlled the reactor pressure and the flow of H_2 or N_2 and measured the H_2 consumed in the reaction. Typically, 2 g of catalyst was added with 300 ml of 2,2,4-trimethylpentane to the reactor vessel, and an in situ reduction was performed by sparging H_2 ($280\ cm^3\ min^{-1}$) through this mixture for 30 min while stirring at 800 rpm. During this time, the vessel was heated to the reaction temperature. Then 2.1 g (0.0196 mol) of *p*-toluidine (Sigma–Aldrich, 99.7%) was added to 50 ml of 2,2,4-trimethylpentane (Lancaster Synthesis, 99%) and heated gently to 323 K, until all of the *p*-toluidine was dissolved. Immediately after the reduction process, this solution was injected into the reactor vessel and stirred at 800 rpm for 5 s to allow mixing. The stirrer was turned off and the vessel was purged with N_2 twice at a flow rate of $280\ cm^3\ min^{-1}$ before being pressurised with N_2 to 1 barg. A 2.5-ml sample was obtained. The vessel was depressurised before being purged with H_2 twice at a flow rate of $280\ cm^3\ min^{-1}$, then pressurised with H_2 to 2 barg. Once the vessel was pressurised, the stirrer was set to 1000 rpm, corresponding to $t = 0$. The reaction was monitored by 2.5-ml gas chromatography (GC) samples obtained at regular time intervals and by H_2 uptake. All gases were $\geqslant$99.995% purity (BOC).

2.3. Analysis

GC was carried out on the liquid samples using a Varian 3400 device equipped with an 8200 CX autosampler, a DB-5 WCOT GC column, and a flame ionisation detector. The *cis* and *trans* isomers of 4-methylcyclohexylamine were identified by cross-referencing their GC peaks with ^1H nuclear magnetic resonance (NMR) using a Bruker Spectrospin 400 Ultrashield device. This was done using a standard of *cis* + *trans* 4-methylcyclohexylamine (Sigma–Aldrich, 97%) by identifying which isomer was present in the largest amount by ^1H NMR (the *trans* and *cis* isomers are identifiable by ^1H NMR), and comparing this with the corresponding gas chromatogram.

p-Toluidine conversion ($\chi_{p\text{-tol}}$) and 4-methylcyclohexylamine selectivity (S_{MCYA}) were calculated using the correlations:

Table 1
Catalyst and support characterisation data

Catalyst	Rhodium *SA* ($m^2\ g^{-1}$)	Dispersion (%, ±4)	Average metal crystallite size diameter (nm)	Surface area ($m^2\ g^{-1}$)	Pore volume ($ml\ g^{-1}$)	Average pore diameter (Å)	Average particle size (μm)
Rh43/Si1a	4.7	43	2.6	321	1.06	132	24.0
Rh41/Si1b	4.5	41	2.7	321	1.06	132	49.9
Rh32/Si1c	3.5	32	3.5	321	1.06	132	96.3
Rh50/Si1d	5.5	50	2.2	321	1.06	132	241.0
Rh37/Si2	4.1	37	3.0	348	1.21	139	10.2
Rh94/Si3	10.3	94	1.2	344	0.96	111	9.5
Rh60/Si4	6.6	60	1.8	488	0.78	64	10.0
Rh71/Si5	7.8	71	1.6	594	0.35	24	10.7

$$\chi_{p\text{-tol}} = \frac{[p\text{-tol}]_0 - [p\text{-tol}]_t}{[p\text{-tol}]_0} \times 100$$

and

$$S_{\text{MCYA}} = \frac{[\text{MCYA}]_t}{[p\text{-tol}]_0 - [p\text{-tol}]_t} \times 100,$$

where $[p\text{-tol}]_t$ and $[\text{MCYA}]_t$ represent *p*-toluidine and 4-methylcyclohexylamine concentration at time t, respectively. The metal crystallite size was calculated from metal surface area and metal loading data with the assumption of hemispherical active rhodium sites and an atomic cross section of 7.52×10^{-20} m^2 atom [14].

3. Results

3.1. Reaction products

The typical reaction profile for the stirred tank reaction showed a nonlinear decrease in *p*-toluidine concentration and a nonlinear increase in 4-methylcyclohexylamine concentration, as shown in Fig. 1. As *p*-toluidine conversion increased, 4-methylcyclohexylamine selectivity increased, typically reaching a selectivity of 60–70%. The *cis* isomer was always produced in greater yields, with the observed *cis*/*trans* ratio decreasing slightly as the reaction proceeded (Fig. 1). The ratio settled at a value of around 1.5.

4-MCYA selectivity was never 100%, due to the formation of various byproducts, mainly bis(4-methylcyclohexyl)amine. Because bis(4-methylcyclohexyl)amine was commercially unavailable, no quantification of this product was performed; however, its presence was confirmed by GC-mass spectroscopy (MS). Ammonia was a byproduct of this dimer formation and was presumed to be produced in an equal ratio to the dimer. Trace amounts of 4-methylcyclohexanol and 4-methylcyclohexanone were also detected during the reaction.

3.2. Mass transfer limitations

A series of tests were performed to examine whether mass transfer effects were influencing the kinetic data. To study whether gas–liquid mass transfer was controlling, the reactor stirrer speed was varied between 600 and 1400 rpm. The resulting H_2 consumption rate was almost identical for each reaction, with values of 0.555 ± 0.030 mmol min^{-1} g^{-1}, indicating that gas–liquid mass transfer did not control the system. A study with double the catalyst mass gave a first-order dependency indicating the absence of liquid–solid mass transfer control. Internal mass transfer or pore diffusion limitations were studied by crushing catalyst Rh50/Si1d, which had an average particle size of 241 μm, to a particle size of <125 μm. The results thus obtained gave identical rates, signifying no pore diffusion limitations. Based on the observations presented above the reactions were assumed to be under kinetic control at reactor stirrer speeds >600 rpm and with catalysts with average particle sizes of ⩽241 μm combined with average pore diameters of ⩾13.2 nm (i.e., catalysts Rh43/Si1a, Rh41/Si1b, Rh32/Si1c, Rh50/Si1d, and Rh37/Si2).

All catalysts had average particle sizes of ⩽241 μm; however, catalysts based on silicas-3, 4, and 5 had average pore diameters of <13.2 nm (Table 1). Tests with these catalysts are addressed later.

3.3. 4-Methylcyclohexylamine as substrate

4-Methylcyclohexylamine was used as the substrate to examine side-product formation. No side products were produced, indicating bis(4-methylcyclohexyl)amine was not formed through the coupling of two 4-methylcyclohexylamine molecules. There was a slight drop in 4-methylcyclohexylamine concentration; however, because no other species were detected, this was determined to be due to adsorption on catalyst (Fig. 2). Concomitant with the drop in 4-methylcyclohexylamine concentration was a slightly increased 4-methylcyclohexylamine *cis*/*trans* ratio, indicating that the *trans* isomer was preferentially adsorbed on the catalyst over the *cis* isomer.

3.4. Influence of p-toluidine concentration

An investigation of *p*-toluidine concentration on the reaction rate was carried out at *p*-toluidine concentrations of 0.028,

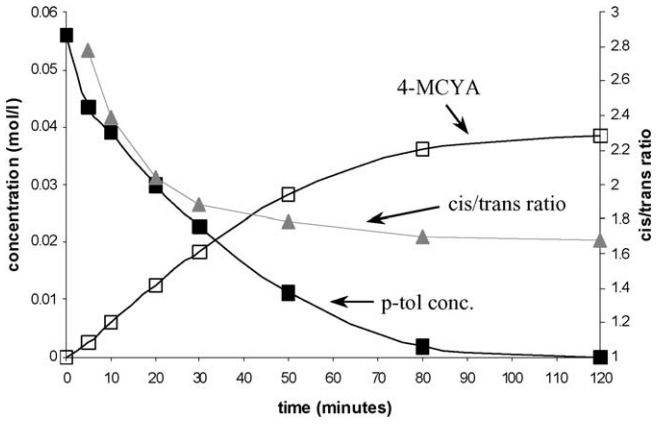

Fig. 1. Typical reaction profile of *p*-toluidine hydrogenation reaction (◆) *p*-toluidine concentration, (□) 4-methylcyclohexylamine concentration, and (▲) 4-methylcyclohexylamine *cis*/*trans* ratio.

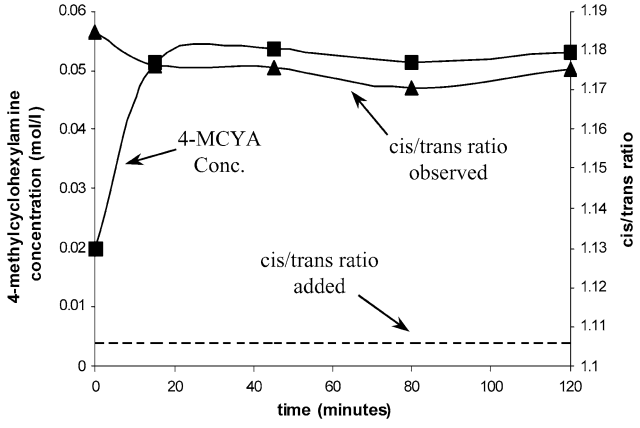

Fig. 2. Data from reaction using 4-methylcyclohexylamine as substrate (■) 4-methylcyclohexylamine concentration, (▲) observed 4-methylcyclohexylamine *cis*/*trans* ratio, and (- - -) 4-methylcyclohexylamine *cis*/*trans* ratio added.

0.056, and 0.112 mol L^{-1} using catalyst Rh60/Si4. The effects on 4-methylcyclohexylamine selectivity and the *cis*/*trans* ratio were also investigated. *p*-Toluidine concentration was shown to have no role in determining the initial reaction rate, indicative of a reaction of zero order with respect to *p*-toluidine. 4-Methylcyclohexylamine selectivity and *cis*/*trans* ratio were equally unaffected.

3.5. Influence of H_2 partial pressure

Different hydrogen partial pressures (1.51, 3.01, and 5.01 bar) were tested using catalyst Rh37/Si2 to examine the influence on the reaction rate. A simple power law model, rate = $k(P_{H_2})^x[p\text{-tol}]^y$, where k is the rate constant, x is the reaction order with respect to hydrogen, and y is the reaction order with respect to *p*-toluidine (zero in this case), was used. A value for x of 1.18 ± 0.22 was obtained. As with *p*-toluidine concentration, hydrogen partial pressure did not influence 4-methylcyclohexylamine selectivity or *cis*/*trans* ratio.

3.6. Metal crystallite size dependency

By using catalysts based on silica-1, which had identical surface areas and pore structures, metal crystallite size dependency could be investigated without interference from pore diameter effects. Because the catalysts had different metal surface areas, the turnover frequencies (TOFs), as opposed to reaction rates, were compared. The TOFs were calculated by

$$\text{TOF} = \frac{n_{H_2}\text{reacted}}{n_{Rh}},$$

where n_{H_2}reacted is the number of moles of H_2 reacted per minute per gram of catalyst and n_{Rh} is the number of moles of active rhodium per gram of catalyst.

A plot of average metal crystallite size with respect to TOF revealed a linear increase in TOF with increasing metal crystallite size (Fig. 3). Regression analysis gave an R^2 value of 0.9989. However, a plot of metal crystallite size versus observed *cis*/*trans* ratio revealed no relationship.

3.7. Effect of catalyst particle size

Once the metal crystallite size effect was known and could be compensated for, catalyst particle size could be investigated more thoroughly. Catalysts based on silica-1 were tested, with the observed reaction rates normalised to a metal crystallite size diameter of 1 nm. As expected, the silica particle size did not alter the TOF (1.81 ± 0.05 min^{-1}), confirming the absence of pore diffusion limitations. The pore diffusion test with catalyst Rh50/Si1d and a crushed form revealed that although *p*-toluidine conversion and 4-methylcyclohexylamine selectivity were unaltered, the observed *cis*/*trans* ratio at *p*-toluidine conversions <100% were different, such that the smaller particle sizes gave a higher *cis*/*trans* ratio. Catalyst Rh50/Si1d was also compared with the other catalysts based on silica-1 (identical support except for silica particle size); again, an increased *cis*/*trans* ratio was observed with decreasing particle size (Fig. 4).

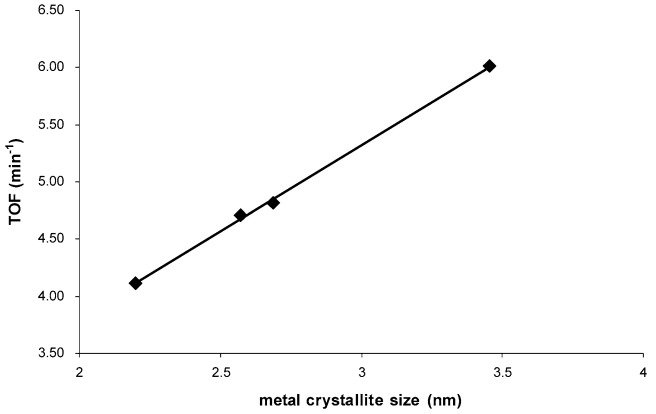

Fig. 3. Effect of metal crystallite size on TOF for catalysts based on silica-1.

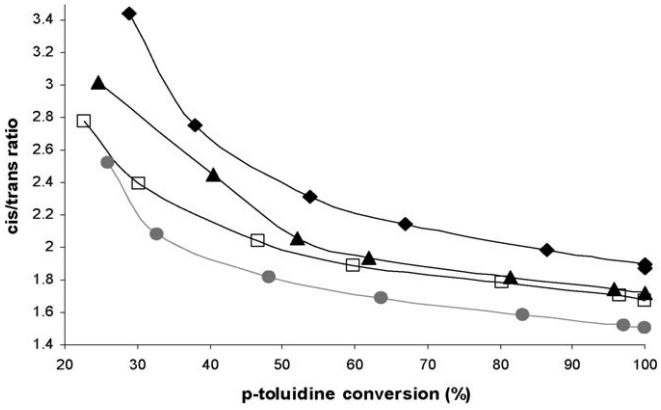

Fig. 4. 4-Methylcyclohexylamine *cis*/*trans* ratio with respect to *p*-toluidine conversion (◆) Rh43/Si1a, (▲) Rh41/Si1b, (□) Rh32/Si1c, and (●) Rh50/Si1d.

3.8. Effect of catalyst pore size

Catalyst pore size was investigated by comparing the results obtained with catalysts prepared from silicas-2–5. Once again, metal crystallite sizes were normalised to 1 nm to decouple their effect on catalyst activity. Pore size had a marked effect on the reaction with catalyst Rh71/Si5, which had the smallest pore diameter (2.4 nm), giving a TOF of 0.99 min^{-1}. Comparing the TOF values for catalysts based on silicas-2–4 (1.91, 1.96, and 2.09 min^{-1}, respectively) clearly shows that increasing the pore diameter to >6.4 nm resulted in only minor increases in TOF, indicating that pore diffusion limitations were negligible in catalysts with pore diameters >6.4 nm. Examination of TOF versus metal crystallite size again revealed a linear increase for catalysts with no pore diffusion limitations; however, catalyst Rh71/Si5 gave a TOF below that of the linear trend, due to the effect of pore diffusion.

4-Methylcyclohexylamine selectivity was unaffected by catalyst pore size; however, there were changes in the observed *cis*/*trans* ratios. Fig. 5 demonstrates that the *cis*/*trans* ratio increased with smaller pore size. In particular, catalyst Rh71/Si5, which had the smallest pore diameter, gave a significant increase compared with the other catalysts.

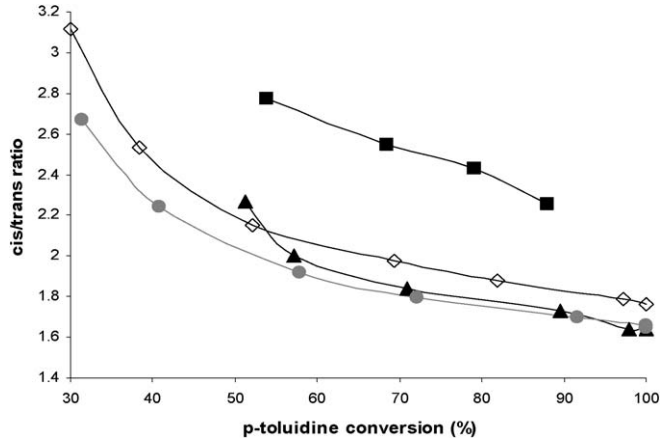

Fig. 5. 4-Methylcyclohexylamine *cis*/*trans* ratio with respect to *p*-toluidine conversion (●) Rh37/Si2, (▲) Rh94/Si3, (◆) Rh60/Si4, and (■) Rh71/Si5.

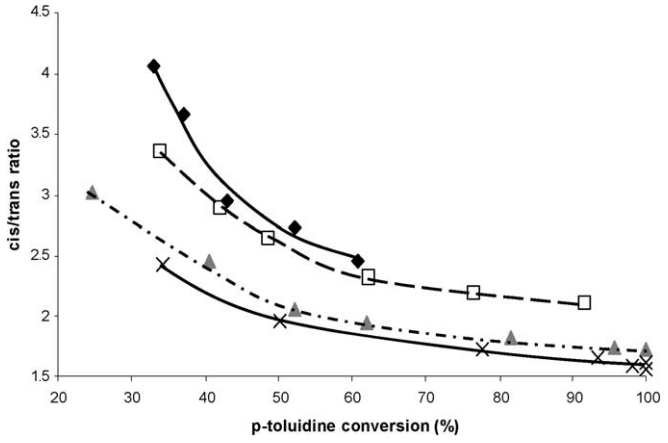

Fig. 6. 4-Methylcyclohexylamine *cis*/*trans* ratio with respect to *p*-toluidine conversion for Rh41/Si1b at (◆) 313 K, (□) 328 K, (▲) 338 K, and (×) 353 K.

Table 2
Activation energies calculated from *cis*-4-methylcyclohexylamine formation and *trans*-4-methylcyclohexylamine formation

Catalyst	E_a (kJ mol^{-1}) (*cis*)	E_a (kJ mol^{-1}) (*trans*)
Rh43/Si1a	54	63
Rh41/Si1b	47	66
Rh32/Si1c	44	62
Rh50/Si1d	41	58
Rh37/Si2	59	58
Rh94/Si3	57	71
Rh60/Si4	53	55
Rh71/Si5	73	90

3.9. Temperature dependency

Experiments were carried out with varying reaction temperatures in the range 313–353 K. Arrhenius plots for *cis*-4-methylcyclohexylamine formation and *trans*-4-methylcyclohexylamine formation were used to calculate the respective apparent activation energies (Table 2). Activation energies calculated from the formation of *cis* and *trans* isomers of 4-methylcyclohexylamine revealed higher values for *trans* over *cis*.

4-Methylcyclohexylamine selectivity did not change with reaction temperature; however, as the activation energies suggest, the *cis*/*trans* ratio was altered. The lower reaction temperatures gave higher *cis*/*trans* ratios for all catalysts. Fig. 6 displays this trend for catalyst Rh41/Si1b.

3.10. Catalyst recycling

Three reactions were performed with reuse of catalyst Rh60/Si4 to investigate whether catalyst deactivation was occurring (Fig. 7). Deactivation did occur as the reaction rate decreased with each catalyst recycle. The largest decrease in rate occurred between using the fresh catalyst and its first recycle, with only a slight decrease evident on the second recycle.

The 4-methylcyclohexylamine *cis*/*trans* ratio changed between the fresh catalyst and the first recycle. At low *p*-toluidine conversion, the *cis*/*trans* ratio was higher with the fresh catalyst than with recycled catalyst, the values becoming closer at

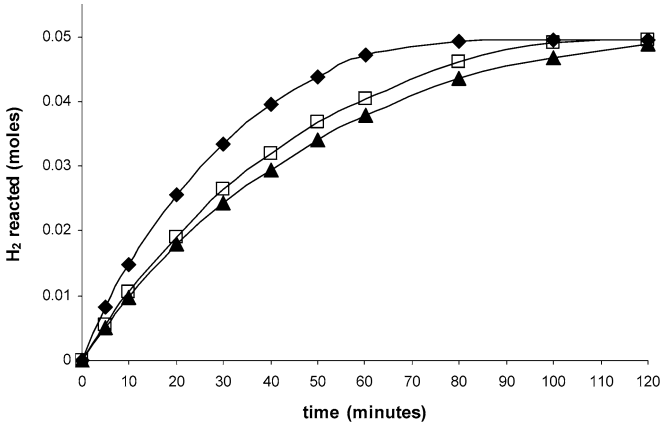

Fig. 7. H_2 uptake profiles for *p*-toluidine hydrogenation with (◆) fresh catalyst, (□) first recycle of catalyst, and (▲) second recycle of catalyst.

p-toluidine conversions >80% (Fig. 8). The first and second recycle produced similar *cis*/*trans* ratios, with the values from the second recycle slightly lower.

4. Discussion

4.1. Product formation

There is no useful literature on the *p*-toluidine hydrogenation reaction; therefore, analogous reactions were examined to reveal useful information concerning product formation. The main product, 4-methylcyclohexylamine, was expected because the equivalent species, cyclohexylamine, was formed during aniline hydrogenation over precious metals [7,8,11–13]. Obviously, aniline hydrogenation could not be used to understand *cis* and *trans* 4-methylcyclohexylamine formation; therefore, the literature of the next most comparable reaction, alkylphenol hydrogenation, was examined. The mechanism of formation of 4-*tert*-butylcyclohexanol from 4-*tert*-butylphenol is via a cyclohexanone intermediate, which is in tautomeric equilibrium with its enol form [15–17]. For *p*-toluidine hydrogenation, it is plausible that the hydrogenation proceeded via enamine/imine intermediate species, which were in tau-

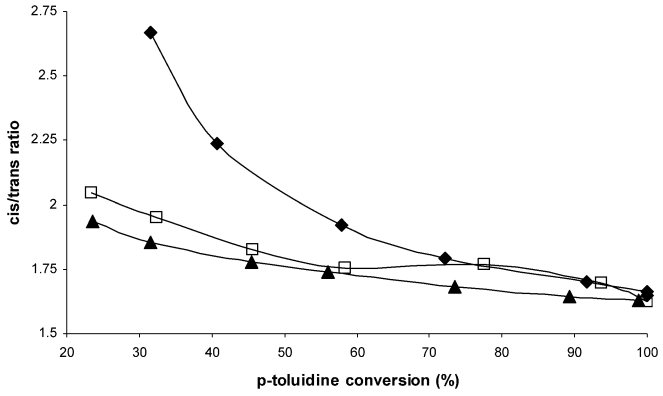

Fig. 8. 4-Methylcyclohexylamine *cis*/*trans* ratio with respect to *p*-toluidine conversion using (◆) fresh catalyst, (□) first recycle of catalyst, and (▲) second recycle of catalyst.

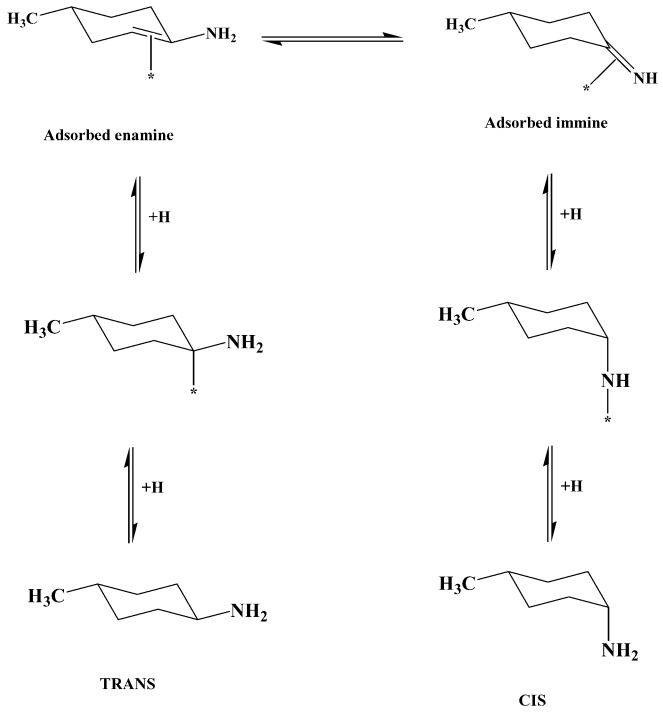

Scheme 1. Pathway to form *cis* and *trans* isomers of 4-methylcyclohexylamine (4-MCYA) through the hydrogenation of *p*-toluidine.

tomeric equilibrium; the *cis* isomer produced via the imine intermediate, and the *trans* isomer produced via the enamine intermediate (Scheme 1). No enamine or imine intermediate was detected in the system at any time, whereas the ketone intermediate has been detected in the substituted phenol hydrogenation over Rh/C [15]. However, this was not unexpected, because imines are known to be highly reactive toward hydrogenation [18], and the C=C bond in an enamine is easily hydrogenated to form an amine [19]. Both *cis* and *trans* isomers have two possible conformations [20,21]; however, they exist almost entirely in conformations shown in Fig. 9. The *cis* isomer was always produced in greater yields than the *trans* isomer, resulting in a *cis*/*trans* ratios >1. The thermodynamic considerations to the resultant *cis*/*trans* ratio are contradictory. *Trans*-4-methylcyclohexylamine is thermodynamically favoured over *cis*-4-methylcyclohexylamine; however, the *trans* isomer is formed via an enamine intermediate, which, when two hydrogen atoms are bonded to the nitrogen atom, is thermodynamically less stable than the imine equivalent [22]. Therefore, the thermodynamically less stable *cis* isomer is produced from the thermodynamically more stable intermediate. Thus the *cis*/*trans* ratio may be determined by the stability, and hence potentially the concentration, of the intermediates. The literature on 4-*tert*-butylphenol hydrogenation revealed similarities. Reactions in *iso*-propanol over a 2% Rh/C catalyst yielded more *cis* isomer than *trans*, with selectivity toward *cis*-4-*tert*-butylcyclohexanol at 80% [23]. A separate study [15] over 5% Rh/C produced *cis*/*trans* ratios between 1.7 and 5.9, depending on the solvent used. In the same study, support effects on the *cis*/*trans* ratio were examined, and it was found that the use of Al_2O_3 or graphite as the support reduced the ratio to between 0.9 and 1.5 for all solvents tested. No study over a Rh/SiO_2 catalyst could be found; however, with alternative supports the *cis* isomer was the favoured product. Reactions using base metals and nonsupported precious metal catalysts gave different results. Over a Ni/Cr_2O_3 catalyst [24], the thermodynamically favourable *trans*-4-*tert*-butylcyclohexanol isomer was produced in a greater yield than the *cis* isomer, giving a *cis*/*trans* ratio of 2.3. This finding is similar to that obtained over a Rh_2O_3 catalyst [16], where again the *trans* isomer was the favoured product.

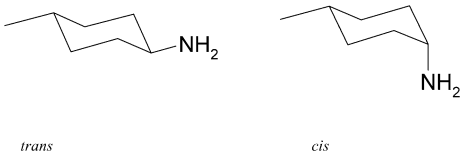

Fig. 9. Conformations of *trans* and *cis* isomers of 4-methylcyclohexylamine.

The major byproduct, bis(4-methylcyclohexyl)amine, was also expected as its equivalent species, dicyclohexylamine was also formed during aniline hydrogenation reactions over similar catalysts [7,8,11–13]. Coupling of a partially hydrogenated imine intermediate and fully hydrogenated 4-methylcyclohexylamine species has been suggested [8] as the route to form dicyclohexylamine in aniline hydrogenation reactions over precious metals. The reaction using 4-methylcyclohexylamine as the reactant produced no bis(4-methylcyclohexyl)-amine, confirming that an intermediate species plays a part in dimer formation. Surface acidity is likely to play a role in bis(4-methylcyclohexyl)amine formation [6]. Although the exact role of the surface acidity is unclear, Ref. [6] shows that in the presence of basic species, dimer formation is hindered. During aniline hydrogenation, the yield of dicyclohexylamine is diminished by adding alkali additives or by using a strongly basic lanthana support [6]. The presence of alkali additives or the use of a basic support is thought to weaken the adsorption of cyclohexylamine, resulting in less side reactions. Mailybaev et al. [12] also showed that the addition of alkali additives decreased byproduct formation during aniline hydrogenation. However, the suggested reason for this was that dicyclohexylamine is formed on the acidic sites of the catalysts; the alkali additives neutralise these acidic sites, causing less byprod-

uct formation. Greenfield [8] demonstrated that the addition of aqueous ammonia to the reaction mixture decreased dicyclohexylamine formation during aniline hydrogenation over a Ru/C catalyst.

The minor species produced in the reaction may be the result of trace water in the solvent. 4-Methylcyclohexanone can be formed from the reaction of water with an enamine intermediate, whereas 4-methylcyclohexanol can be formed by hydrogenation of 4-methylcyclohexanone. The presence of water produces cyclohexanol in aniline hydrogenation [8,12], and the mechanism of formation through the enamine intermediate was suggested by Greenfield [8].

Certain reaction conditions and catalyst physical characteristics altered the rate of product formation and selectivity. The reaction with respect to *p*-toluidine was zero-order; hence *p*-toluidine concentration had no role in determining the initial reaction rate. The hydrogenation of 4-*tert*-butylphenol over Rh/C was also shown to be zero-order in 4-*tert*-butylphenol [25]. The *cis*:*trans* ratio of 4-methylcyclohexylamine was also unaffected by changes in *p*-toluidine concentration.

Increased H_2 pressure resulted in an increase in reaction rate. The reaction order with respect to H_2 concentration was calculated to be 1.18 ± 0.22. This disagrees with literature available on aniline hydrogenation, where it was shown the reaction was zero order in H_2 [13]; however, this result was gained by performing gas–phase reactions at high pressure. Hydrogenation of benzene, and its derivatives, at high pressures are known to be zero-order in both H_2 and aromatic species, due to complete coverage of the catalytic surface by both reactants [17]. At low pressures, the reaction order in H_2 can be greater than zero-order [16,17]. Work performed on 4-*tert*-butylphenol hydrogenation over Rh/C at pressures between 0.2 and 1.0 MPa, was also shown to be positive order with respect to H_2 partial pressure [25]. Due to the positive order in H_2 during *p*-toluidine hydrogenation, the amount of H_2 adsorbed on the catalytic surface is proportional to the reaction rate. Consequently, either H_2 adsorbing on the catalyst or the addition of hydrogen to either *p*-toluidine or a partially hydrogenated intermediate is the rate-limiting step. H_2 pressure did not alter the product distribution; therefore, as with *p*-toluidine concentration, the *cis*:*trans* isomer ratio of the product was unaltered by varying H_2 pressure.

Studies on metal crystallite size revealed antipathetic behaviour or a negative particle size effect (Fig. 3) over the range of crystallite sizes and temperatures (313–353 K) tested; that is, a larger crystallite size produced a higher TOF. Fig. 10 shows the relationship between TOF and metal crystallite size with catalyst Rh94/Si3 data added. This catalyst has a different silica pore size, but it is outwith the diffusional regime. The data from this catalyst extend the relationship down to around 1 nm. Rhodium crystals have a fcc closed packed arrangement; as a fcc crystal increases in size, the number of face surface atoms (C_9^3 sites) increases at the expense of the edge (C_7^9) and corner ($C_4^{9,10}$) sites [26]. This suggests the hydrogenation reaction took place on the plane face surface as opposed to edge and corner sites. There are no analogous studies of metal crystallite size effects on *p*-toluidine or substituted aniline hydrogenations in the literature. However, the antipathetic behaviour displayed is corroborated by the literature on aromatic ring hydrogenation, because the activity of benzene hydrogenation over Rh/Al_2O_3 is low for very small Rh crystals [27]. Moreover, another study of benzene hydrogenation over Rh/Al_2O_3 authors concluded that with catalysts with dispersions between 20 and 90%, there was a decrease in turnover number as dispersion increased (i.e., smaller metal crystals) [28]. Benzene hydrogenation over Pt/Al_2O_3 also displayed decreased TOF with increasing dispersion [29]. Other studies of toluene hydrogenation over platinum and iridium catalysts also revealed similarities to the current study [30,31]. 4-Methylcyclohexylamine selectivity and *cis*/*trans* ratio were not affected by changes in metal crystallite size.

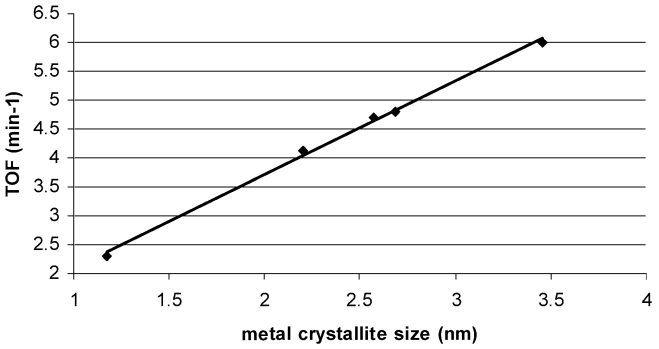

Fig. 10. Effect of metal crystallite size on TOF for catalysts based on silica-1 and Rh94/Si3.

Catalyst pore size affected the TOF such that below a threshold pore diameter, the TOF was perturbed. This threshold pore diameter was <6.4 nm. Pore diameters above this threshold showed only very slight differences in TOF. The perturbation of the rate was due to a diffusion limitation through the catalyst pores. This limitation was a "Knudsen-type" diffusion limitation. Knudsen diffusion is usually described for gas-phase molecules where the mean free path between molecules is larger than the pore diameter of the catalyst; therefore, diffusion of the molecule is interrupted by collisions with the pore wall. In the present case, the reactant molecules diffuse through a liquid, and consequently collisions with the solvent molecule will occur before collisions with the pore walls. But because the pore diameter in catalyst Rh71/Si5 was so narrow (2.4 nm), we propose that some collisions with the pore walls occurred, causing the diffusion limitation; hence the term "Knudsen-type" diffusion. A more quantitative way of examining this diffusion limitation is by examining the diffusivity, D, as diffusion is proportional to the diffusivity of the species. Diffusivity in liquids can be up to 10,000 lower than for gas at atmospheric pressure [32]. The diffusivity in catalyst pores is called the "effective diffusivity," D_e, and is related to the diffusivity by the following equation [33]:

$$D_e = \frac{D\phi\sigma}{\tau},$$

where ϕ is the porosity of the catalyst, defined by the ratio of volume of void space to total volume of catalyst, σ is the constriction factor, which accounts for the variation in the cross-sectional area of the pores, and τ is the tortuosity, defined by

Table 3
Variation of total pore length per gram of catalyst with average pre diameter for each catalyst

Total pore length ($m\,g^{-1}$)	Average pore diameter (Å)	Catalyst
7740	132	Rh43/Si1a
7740	132	Rh41/Si1b
7740	132	Rh32/Si1c
7740	132	Rh50/Si1d
7969	139	Rh37/Si2
9814	111	Rh94/Si3
24,308	64	Rh60/Si4
80,263	24	Rh71/Si5

the actual distance that a molecule travels between two points divided by the shortest distance between two points. First, examining Table 1 reveals that pore volume per gram of catalyst decreased as the average pore diameter decreased, and hence the porosity, ϕ, decreased. Therefore, as the catalyst diameter decreased, the effective diffusivity decreased. Second, applying the equation [32]

$$L = \frac{SA^2}{4\pi V},$$

where L is the total catalyst pore length, SA is the support surface area, and V is the support pore volume, demonstrates that the pore length per gram of catalyst increases as average pore diameter decreases (Table 3). Because the particle sizes of catalysts based on silicas-2–5 were almost identical, the tortuosity of the catalysts increased with increasing pore length per gram of catalyst; thus the effective diffusivity decreased as catalyst pore diameter decreased. Ren et al. [34] showed that tortuosity increased with decreasing pore diameter. The combined influence of these two factors means an overall decrease in the effective diffusivity with decreasing catalyst pore diameter. Below the threshold diameter of 6.4 nm, diffusivity impinged to such an extent to produce diffusion limitations.

The observed *cis*/*trans* ratio changed during all reactions, decreasing over time toward a fixed value. For a simultaneous reaction, if the two competing reactions are of the same kinetic order (as they are in this case), then pore structure does not affect product selectivity [32]. Therefore, the change in ratio was due not to a change in selectivity (i.e., enamine/imine ratio), but rather to the *trans* isomer having a greater affinity for the support than the *cis* isomer. The silica support in this study was acidic; therefore, the basic *cis* and *trans* amines will have an affinity for the silica surface. The greater affinity of the *trans* isomer was proved by the reaction using 4-methylcyclohexylamine as the substrate, which displayed a slightly increased *cis*/*trans* ratio due to the preferential adsorption of the *trans* isomer on the catalyst support. This chromatographic effect of the silica produced a differential in the rate of transport of the *cis* and *trans* isomers through the pores. Consequently, the *cis*/*trans* ratios seen during the initial stages of the reaction represents not the production of *cis* and *trans* isomers at the catalytic site, but rather a modified ratio due to preferential adsorption of the *trans* isomer. The observed *cis*/*trans* ratios decreased as the support became saturated with product until a constant ratio was achieved. The catalyst pore diameter played a role in determining the observed *cis*/*trans* ratio. The smaller pore diameters gave higher *cis*/*trans* ratios at equal *p*-toluidine conversion. Catalyst Rh71/Si5, which had the smallest pore diameter, had the largest support surface area and the longest pore length per gram of catalyst. By comparing catalysts Rh37/Si2 and Rh71/Si5 (the two extreme cases), the increased *cis*/*trans* ratio with decreasing pore diameter can be rationalised in two nonexclusive ways. Because the surface area of catalyst Rh71/Si5 was larger, more *trans* isomer than *cis* isomer may be adsorbed on the support. Moreover, because catalysts Rh37/Si2 and Rh71/Si5 had almost the same particle size, the increase in pore length is analogous to an increase in the length of a chromatographic column, which results in increased separation of species.

It is likely that *p*-toluidine also adsorbed on the support in catalyst Rh71/Si5, contributing to the diffusion limitation observed. But because aromatic amines are less basic than nonaromatic amines, *p*-toluidine would have less affinity for the acidic sites than 4-methylcyclohexylamine and so would be displaced by product.

Catalyst particle size also affected the *cis*/*trans* ratio, with smaller particles demonstrating an increased *cis*/*trans* ratio. This phenomenon was again due to the greater affinity of the *trans* isomer to adsorb on the support. All of the catalysts had the same pore structure, pore length per gram of catalyst, and internal support surface area. The only difference was the external surface area of the catalysts, with the smaller catalyst particle sizes having larger external surface areas. (The surface area measurements were taken from a single batch of support before they were crushed to their corresponding sizes.) As more external surface area was exposed with the smaller particle sizes, the more *trans* adsorption with respect to *cis* occurred, resulting in slight increased observed *cis*/*trans* ratios.

Reaction temperature changed the *cis*/*trans* ratio produced in the reaction. Decreasing the reaction temperature increased the *cis*/*trans* ratio. This is in keeping with the activation energies calculated from the rate of formation of each isomer. Overall, the activation energies calculated from *trans* isomer formation were larger than those calculated from *cis* isomer formation, reinforcing the proposed mechanism that the *cis* and *trans* isomers are produced from different intermediates—an imine and enamine, respectively.

Catalyst deactivation was evident on catalyst recycling. The most significant drop in catalyst activity was between the reaction using fresh catalyst sample and the reaction with the first reuse of this sample. The second reuse of the catalyst produced a slight drop in activity, indicating that deactivation was an ongoing process that increasingly deactivated the catalyst. References [6–8,13] states that both aniline and cyclohexylamine act as inhibitors in aniline hydrogenation. The basic lone pair on the nitrogen atom forms a strong bond to the active metal; therefore, it is likely that 4-methylcyclohexylamine inhibited *p*-toluidine hydrogenation, with contributions from bis(4-methylcyclohexyl)amine and ammonia. The catalyst recycling experiments produced evidence corroborating the chromatography effect, producing different *cis*/*trans* ratios. On the second

and third recycles, no sharp decrease in *cis*/*trans* ratio occurred, as was observed with the fresh catalyst. Because the used catalysts have already been exposed to 4-methylcyclohexylamine from the previous reaction(s), the acidic sites have been neutralised to such an extent that any chromatographic effect is diminished.

5. Conclusion

We have shown that the hydrogenation of *para*-toluidine over Rh/silica exhibits an antipathetic particle size effect, suggesting that plane face surface atoms, such as C_9^3 sites, are the active site for ring hydrogenation. The reaction is zero order in *p*-toluidine and first order in hydrogen, with the likely mechanism of formation of the *cis* and *trans* isomers through surface imine and enamine intermediates. The support was also shown to play a part, adsorbing *trans*-4-MCYA in the early stages of the reaction and resulting in a varying *cis*:*trans* ratio. The effect of pore size was also studied; a dramatic decrease in activity was observed at pore diameter <6.4 nm.

Acknowledgments

The authors acknowledge the support of the EPSRC and the following companies: Johnson Matthey, Grace Davison, Robinson Brothers, BP-Amoco, and Accelerys, as part of the Innovative Manufacturing Initiative (IMI).

References

[1] H. Blaser, A. Indolese, A. Schnyder, H. Steiner, M. Studer, J. Mol. Catal. A Chem. 173 (2001) 3.
[2] R.A. Sheldon, R.S. Downing, Appl. Catal. A Gen. 189 (1999) 163.
[3] M. Freifelder, G.R. Stone, J. Org. Chem. 27 (1962) 3568.
[4] V.S. Ranade, R. Prins, J. Catal. 185 (1999) 479.
[5] J.M. Devereux, K.R. Payne, E.R.A. Peeling, J. Chem. Soc. (1957) 2845.
[6] G. Mink, L. Horváth, React. Kinet. Catal. Lett. 65 (1998) 59.
[7] E.L. Pitara, B. N'Zemba, J. Barbier, F. Barbot, Miginiac, J. Mol. Catal. A Chem. 106 (1996) 235.
[8] H. Greenfield, J. Org. Chem. 29 (1964) 3082.
[9] S. Narayanan, R. Unnikrishnan, V. Vishwanathan, Appl. Catal. A Gen. 129 (1995) 9.
[10] S. Narayanan, R. Unnikrishnan, J. Chem. Soc. Faraday Trans. 93 (1997) 2009.
[11] V. Vishwanathan, S. Narayanan, J. Chem. Soc. Commun. (1990) 78.
[12] B.T. Mailyubaev, A. Ualikhanova, Russ. J. Appl. Chem. 66 (1994) 1739.
[13] D.V. Sokolskii, A. Ualikhanova, A.E. Temirbulatova, React. Kinet. Catal. Lett. 20 (1982) 35.
[14] P.A. Webb, C. Orr, Analytical Methods in Fine Particle Technology, Micrometrics Instrument Corporation, Norcross, GA, 1997, p. 260.
[15] K.G. Griffin, S. Hawker, P. Johnston, M.-L. Palacios, C. Clayton, D.G. Morrell (Eds.), Catalysis of Organic Reactions, Dekker, New York, 2002, p. 529.
[16] S.R. Konuspaev, K.N. Zhanbekov, N.V. Kul'kova, D.Y. Murzin, Chem. Eng. Technol. 20 (1997) 144.
[17] D.T. Murzin, S.R. Konuspaev, Kinet. Catal. 33 (1992) 434.
[18] B.W. Hoffer, P.H.J. Schoemakers, P.R. Mooijman, G.M. Hamminga, R.J. Berger, A.D. van Langeveld, J.A. Moulijn, Chem. Eng. Sci. 59 (2004) 259.
[19] Y.Y. Huang, W.M.H. Sachtler, Appl. Catal. A Gen. 182 (2) (1999) 365.
[20] H. Booth, G.C. Gidley, P.R. Thornburrow, J. Chem. Soc. B (1971) 1047.
[21] H. Booth, Progr. NMR Spectrosc. 5 (1969) 149.
[22] J. March, M.B. Smith, Advanced Organic Chemistry, Mechanism, Reactions and Structure, Wiley, New York, 2001, p. 77.
[23] G.D. Yadav, P.K. Goel, J. Mol. Catal. A Chem. 184 (2002) 281.
[24] D.Y. Murzin, S.R. Konspaev, Catal. Today 79–80 (2003) 229.
[25] G.D. Yadav, P.K. Goel, J. Mol. Catal. A Chem. 184 (2002) 281.
[26] M. Che, C.O. Bennet, Adv. Catal. 36 (1989) 55.
[27] G.A. Del Angel, B. Coq, G. Ferrat, F. Figueras, S. Fuentes, Surf. Sci. 156 (1985) 943.
[28] S. Fuentes, F. Figueras, J. Catal. 61 (1980) 443.
[29] F. Flores, R.L. Burwell Jr, J.B. Butt, J. Chem. Soc. Faraday Trans. 88 (8) (1992) 1191.
[30] A.D. Chandler, A.B. Schabel, L.H. Pignolet, J. Phys. Chem. B 105 (2001) 149.
[31] Z. Hu, F.S. Xiao, S.K. Purnell, O. Alexeev, S. Kawi, S.E. Deutsch, B.C. Gates, Nature 372 (1994) 346.
[32] A. Wheeler, Adv. Catal. 3 (1951) 249.
[33] H.S. Fogler, Elements of Chemical Reaction Engineering, Prentice Hall, Englewood Cliffs, NJ, 1999, p. 739.
[34] X.-H. Ren, M. Bertmer, S. Stapf, D.E. Demco, B. Blümich, C. Kern, A. Jess, Appl. Catal. A Gen. 228 (2002) 39.